Adsorption of Carbon Tetrachloride on Graphitized Thermal Carbon Black and in Slit Graphitic Pores: Five-Site versus One-Site Potential Models

D. D. Do* and H. D. Do

Department of Chemical Engineering, University of Queensland, St. Lucia, Qld 4072, Australia

Received: December 11, 2005; In Final Form: February 28, 2006

The performance of intermolecular potential models on the adsorption of carbon tetrachloride on graphitized thermal carbon black at various temperatures is investigated. This is made possible with the extensive experimental data of Machin and Ross[1], Avgul et al.,[2] and Pierce[3] that cover a wide range of temperatures. The description of all experimental data is only possible with the allowance for the surface mediation. If this were ignored, the grand canonical Monte Carlo (GCMC) simulation results would predict a two-dimensional (2D) transition even at high temperatures, while experimental data shows gradual change in adsorption density with pressure. In general, we find that the intermolecular interaction has to be reduced by 4% whenever particles are within the first layer close to the surface. We also find that this degree of surface mediation is independent of temperature. To understand the packing of carbon tetrachloride in slit pores, we compared the performance of the potential models that model carbon tetrachloride as either five interaction sites or one site. It was found that the five-site model performs better and describes the imperfect packing in small pores better. This is so because most of the strength of fluid−fluid interaction between two carbon tetrachloride molecules comes from the interactions among chlorine atoms. Methane, although having tetrahedral shape as carbon tetrachloride, can be effectively modeled as a pseudospherical particle because most of the interactions come from carbon−carbon interaction and hydrogen negligibly contributes to this.

1. Introduction

Adsorption of gases or vapors on solid surfaces such as the graphitized thermal carbon black (GTCB) has been extensively studied in the literature[4−11] because such a material if graphitized adequately can yield a very homogeneous surface.[12−13] This material is, therefore, often used as a reference material for characterization of the interaction between a molecule and surface carbon atoms. Adsorption of simple gases, such as noble gases and hydrocarbons, on GTCB has been substantially studied in the literature.[6] However, for chlorinated hydrocarbons such as carbon tetrachloride, work has been limited. Therefore, it is important to investigate the performance of various intermolecular potential models in the description of vapor−liquid equilibria data and to study the adsorption of carbon tetrachloride on carbon black surface by using the grand canonical Monte Carlo (GCMC) simulation method.[14−16] The physical properties of carbon tetrachloride are listed in Table 1. For comparison, we also compared these properties with methane, carbon dioxide, and benzene. Like these species, carbon tetrachloride does not have a dipole.

2. Theory

To simulate the adsorption isotherms, we used the grand canonical Monte Carlo simulation, first proposed by Norman and Filinov.[14] This simulation technique is described in detail in a number of books,[15−16] and here we summarize the essential points that we used in our simulations. To simulate the carbon black surface, we used a simulation box, the bottom of which is the graphite surface, while the top of the box is a hard wall.

2.1. Multisite Potential Model. Because of the tetrahedral shape of carbon tetrachloride, it should not be treated as a single interaction site particle because, in the confined space of pores, the molecular shape is very important in the structure of adsorbed phase and the packing density. Moreover, most of the strength of interaction between two carbon tetrachloride molecules comes from the interactions of chlorine atoms that are located at the vertexes of a tetrahedral. Therefore, the shape is important, and hence, the potential model must reflect that. We consider carbon tetrachloride as a particle composed of interaction sites to properly model the molecular shape. Each site on one molecule will interact with all sites of another molecule. We write below the interaction energy between a site "*a*" on a molecule "*i*" with a site "*b*" on a molecule "*j*" with a Lennard−Jones 12−6 equation:

$$\varphi_{i,j}^{(a,b)} = 4\epsilon^{(a,b)}\left[\left(\frac{\sigma^{(a,b)}}{r_{i,j}^{(a,b)}}\right)^{12} - \left(\frac{\sigma^{(a,b)}}{r_{i,j}^{(a,b)}}\right)^{6}\right] \qquad (1)$$

The subscript is used for the particle, while the superscript is for the site. Thus, for a given intersite distance $r_{i,j}^{(a,b)}$ to calculate the interaction energy $\varphi_{i,j}^{(a,b)}$, we need to know the cross collision diameter $\sigma^{(a,b)}$ and the cross well depth $\epsilon^{(a,b)}$. They can be determined by invoking the mixing rule due to Lorentz−Berthelot (LB),

$$\sigma^{(a,b)} = \frac{[\sigma^{(a,a)} + \sigma^{(b,b)}]}{2}$$

and

$$\epsilon^{(a,b)} = \sqrt{\epsilon^{(a,a)}\epsilon^{(b,b)}}$$

Knowing the site−site interaction, the interaction between two

* Corresponding author. E-mail: duongd@cheque.uq.edu.au. Telephone: +61-7-3365-4154. Fax: +61-7-3365-2789.

10.1021/jp057230q CCC: $33.50
Published on Web 04/22/2006

TABLE 1: Properties of Carbon Tetrachloride

	units	carbon tetrachloride	methane	benzene	carbon dioxide
T_c	K	556.4	190.6	562.1	304.2
P_c	Pa	4.56×10^6	4.6×10^6	4.894×10^6	7.376×10^6
V_c	m^3/kmol	0.276	0.099	0.259	0.094
T_b	K	349.7	111.7	353.3	194.7
T_{tr}	K	250.33	90.67	278.7	216.6
P_{tr}	Pa		11,700	4.785×10^3	5.736×10^5
quadrupole moment	C m^2	0	0	-23.9×10^{-40}	-14.9×10^{-40}
dipole	D	0	0	0	0

molecules is simply (assuming pairwise additivity)

$$\varphi_{i,j} = \sum_{a=1}^{M} \sum_{b=1}^{M} \varphi_{i,j}^{(a,b)}$$

where M is the number of sites on each molecule.

There are a number of intermolecular potential models for carbon tetrachloride that have been proposed in the literature. They range from the simple single-site LJ model to complex models that account for five interaction sites involving both dispersive and electrostatic forces. For the five-site models, which treat carbon tetrachloride as a tetrahedral with the carbon atom at its center and four chlorine atoms at the four vertexes, the carbon−chloride bond length is 1.766 Å. The molecular parameters of carbon and chlorine atoms of two potential models are listed in the following table. One is proposed by McDonald et al.,[17] and the other is by Adan and co-workers.[18] The

	carbon atom		chlorine atom	
	σ (Å)	ϵ/k (K)	σ (Å)	ϵ/k (K)
McDonald model	4.6	51.2	3.5	102.4
Adan model	4.6	39	3.4	120
this work	4.6	39	3.5	105

McDonald (M) model and the Adan (A) model are derived from the analysis of liquid properties, and therefore, we expect that they do not perform well in the description of vapor−liquid equilibria, which we argue must be a prerequisite for the description of adsorption isotherm. To test for their abilities to describe VLE, we apply the standard Gibbs ensemble Monte Carlo simulation.[15] This will be discussed in the Results and Discussion Section.

2.2. Solid−Fluid Potential. For a polyatomic molecule with M centers of the LJ type, the solid fluid interaction energy can be determined as follows. The interaction potential energy between a site a of the molecule i and the homogeneous flat solid substrate is calculated by the 10−4−3 Steele potential.[19−20] It takes the following form:

$$\varphi_{i,s}^{(a)} = 4\pi\rho_C\epsilon^{(a,s)}[\sigma^{(a,s)}]^2\Delta\left\{\frac{1}{5}\left(\frac{\sigma^{(a,s)}}{z_i^{\,a}}\right)^{10} - \frac{1}{2}\left(\frac{\sigma^{(a,s)}}{z_i^{\,a}}\right)^{4} - \frac{[\sigma^{(a,s)}]^4}{6\Delta(0.61\Delta + z_i^{\,a})^3}\right\} \quad (2)$$

where ρ_c is the volumetric carbon atom density (114 nm^{-3}), and Δ is the spacing between the two adjacent graphite layers (0.3354 nm). The solid−fluid molecular parameters, the collision diameter $\sigma^{(a,s)}$, and the interaction energy $\epsilon^{(a,s)}$ are calculated from the Lorentz−Berthelot mixing rule. The solid−fluid interaction energy is usually adjusted with the introduction of the solid−fluid binary interaction parameter, k_{sf}, such that the experimental Henry constant is reproduced by the GCMC simulations, that is

$$\epsilon^{(a,s)} = (1 - k_{sf})\sqrt{\epsilon^{(a,a)}\epsilon^{(s,s)}}$$

For simplicity, we will assume that the binary interaction parameter, k_{sf}, is the same for all interaction sites of a molecule. Having the interaction potential energy of the site "a" of the molecule "i" with the surface as given in eq 2, the solid−fluid interaction energy of the molecule "i" is simply

$$\varphi_{i,s} = \sum_{a=1}^{M} \varphi_{i,s}^{(a)}$$

Once the solid−fluid potential energy for one wall is obtained, the potential energy between one molecule with a pore of slit shape is $\varphi_{i,p} = \varphi_{i,s}(z) + \varphi_{i,s}(H - z)$, where H is the physical pore width. It is defined as the distance between the plane passing through carbon atoms of the outermost layer of one wall to the corresponding plane of the other wall.

Having defined the fluid−fluid and solid−fluid interaction, we describe briefly next the various ensembles that we use in our investigation of vapor−liquid equilibria and adsorption. For VLE, we apply the standard Gibbs ensemble Monte Carlo, which was first suggested by Panagiotopoulos and co-workers[21] and use the Rosenbluth scheme for insertion and removal (details can be found in Frenkel and Smith[15]), while for adsorption, we use the grand canonical Monte Carlo (GCMC) simulation. The parameters used in the GCMC simulation are (i) the box length in the case of slit pore is at least 10 times the collision diameter (for low pressures where the adsorbed density is low, we use the box length as high as 60 times the collision diameter), (ii) the cutoff radius is half of the box length, and (iii) the number of cycles for the equilibration step is 20 000, and that for the statistics collection is also 20 000.

2.3. Isosteric Heat. The heat of adsorption (energy released per unit increment number of molecule added to the adsorbed phase) can be obtained directly from the simulation. It is the difference between the molar enthalpy of adsorbate in the vapor phase and the partial molar enthalpy of the adsorbed phase ($\bar{h}_a = (\partial H_a/\partial N_a)_{P,T}$) (this is the isosteric heat):

$$-\Delta h = h_G - \bar{h}_a$$

By definition, the molar enthalpy of a given phase is the sum of the molar internal energy and the product of pressure and molar volume of that phase. For carbon tetrachloride at temperatures considered in this paper, the bulk gas pressure is generally very low, and therefore, the gas phase can be treated as an ideal gas. Thus $h_G = e_G + pv_G \approx e_G + R_gT$. For the adsorbed phase, its molar volume is assumed to be negligible compared to that in the gas phase, so the change in the molar enthalpy of the above equation is $-\Delta h = R_gT + e_G - \bar{e}_a$. If we assume that the kinetic energy of adsorbate remains the same between the two phases (this approximation is reasonable as

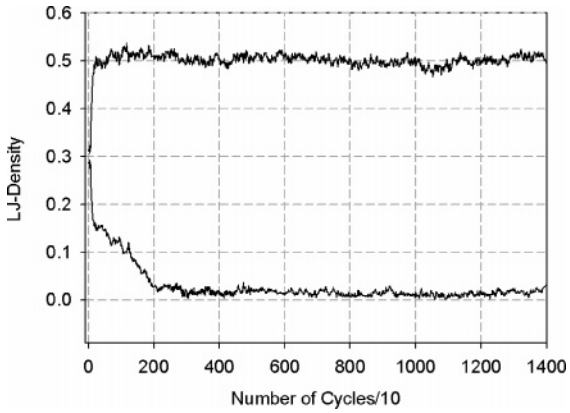

Figure 1. Evolution of densities of the two boxes.

long as the temperature is not extremely low), the heat of adsorption is simply the difference between the potential energy of the vapor phase and that in the adsorbed phase $-\Delta h = R_g T + u_G - \bar{u}_a$. The potential energy is readily calculated in the course of GCMC simulation. For example, the molar potential energy of the vapor phase is calculated as the partial derivative of the total potential energy of the vapor phase with respect to the total number of particle, i.e., $u_G = \partial\langle U_G\rangle/\partial\langle N\rangle$. Similarly, $\bar{u}_a = \partial\langle U_a\rangle/\partial\langle N\rangle$. Applying the fluctuation theory,[22] the change in the molar enthalpy is:

$$-\Delta h = R_g T - \frac{\langle U_{a,ext} N\rangle - \langle U_{a,ext}\rangle\langle N\rangle}{\langle N^2\rangle - \langle N\rangle^2} \tag{3a}$$

where $U_{a,ext}$ is the potential energy between adsorbate molecules plus that between adsorbate molecule and the solid substrate. This equation was first derived by Nicholson and Parsonage.[16] To distinguish the contributions of fluid−fluid interaction and fluid−solid interaction, we rewrite the above equation as:

$$-\Delta h = \left[R_g T - \frac{\langle U_{a,ff} N\rangle - \langle U_{a,ff}\rangle\langle N\rangle}{\langle N^2\rangle - \langle N\rangle^2}\right] - \frac{\langle U_{a,sf} N\rangle - \langle U_{a,sf}\rangle\langle N\rangle}{\langle N^2\rangle - \langle N\rangle^2} \tag{3b}$$

The square bracket term in the above equation is the contribution of fluid−fluid interaction to the isosteric heat of adsorption, while the last term is the contribution from the fluid−solid interaction.

3. Results and Discussion

3.1. Gibbs Ensemble Monte Carlo Simulation. Before discussing the adsorption of carbon tetrachloride on graphitized thermal carbon black, we carry out the Gibbs ensemble Monte Carlo simulation to test the suitability of the various potential models on the description of vapor−liquid equilibria. Figure 1 shows a typical plot of the densities of the two boxes as a function of cycle. Starting with the same density in both boxes, the system quickly splits into two densities.

We start this type of simulation with the Adan model,[18] and the results of the Adan model for 450 and 500 K are shown in Figure 2 as plot of temperature vs the saturation density and in Figure 3 as vapor pressure vs temperature. The experimental data is presented as unfilled circles, while the results with the Adan model are shown as triangles. It is seen that the Adan model underpredicts the vapor saturation density, while it overpredicts the liquid saturation density. Furthermore, the Adan model significantly underpredicts the saturation vapor pressure, suggesting that this model is not suitable for the adsorption

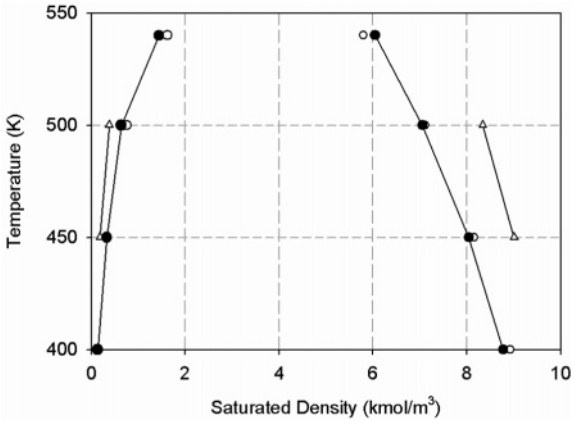

Figure 2. Plot of the temperature vs saturation density (unfilled circle: experimental data; triangles: Adan model; filled circles: model proposed in this work).

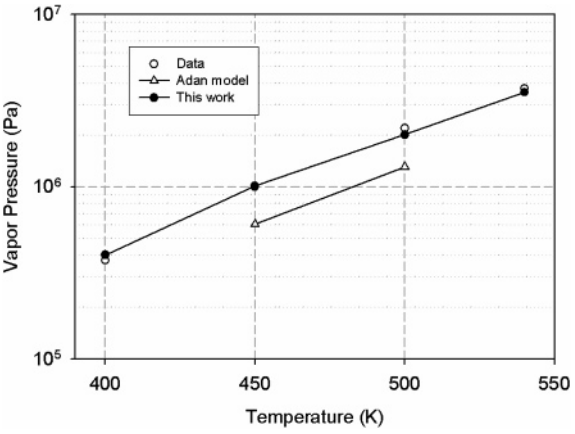

Figure 3. Plot of the saturation vapor pressure vs temperature (unfilled circle: experimental data; triangles: Adan model; filled circles: model proposed in this work).

study. The same conclusion is also derived for the potential model of McDonald and co-workers.

The Adan model gives a too-high saturation liquid density, suggesting that the collision diameter of chlorine ($\sigma = 3.4$ Å) is low. Furthermore, it gives a too-low saturation vapor pressure, indicating that the well depth of chlorine is too high ($\epsilon/k_B = 120$ K). To remedy this, we increase the collision diameter of chlorine to 3.5 Å and perform the optimization to determine its well depth as 105 K. With the new set of molecular parameters for carbon and chlorine obtained in this work (tabulated in Table 1), the saturation vapor and liquid densities and vapor pressure are obtained from the Gibbs ensemble Monte Carlo and shown in Figures 2 and 3 as filled circles, and we see that the new model describes the VLE data well.

3.2. Adsorption of Carbon Tetrachloride on GTCB. In the GCMC simulations of adsorption on graphitized thermal carbon black, we obtain the number of particles in the simulation box for a given temperature, volume, and chemical potential. In presenting the results, we plot them as (i) surface excess vs pressure, (ii) a two-dimensional (2D) plot of local density vs the distance above the surface, and (iii) a three-dimensional (3D) plot of local density vs the distance above the surface and the angle formed between the vector joining the carbon atom and one of the chlorine atoms and the z direction (perpendicular to the pore surface). The average surface excess is defined as

$$\Gamma_{av} = \frac{\langle N\rangle}{L_x L_y} - \frac{\rho L_x L_y H'}{L_x L_y} \tag{4}$$

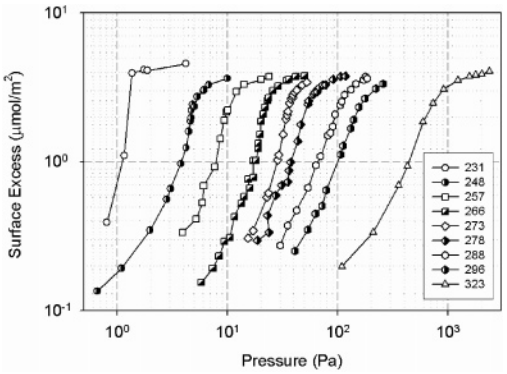

Figure 4. Composite experimental data of Machin and Ross[1] at various temperatures.

where ρ is the bulk molecular density, L_x and L_y are the box lengths in the x and y directions, respectively, $\langle N \rangle$ is the ensemble average of the number of particle in the simulation box, and H' is the *accessible pore width*. The latter is defined as the width that is accessible to carbon tetrachloride molecule. This is done as follows. The volume space that is accessible to the center of mass (COM) of a particle is defined as the space in which the solid−fluid potential energy is less than zero. This is done in a similar way to that of Kaneko et al.,[23] who dealt with a 1C-LJ particle. Thus, if we define z_0 as the distance (from the carbon surface to the COM of carbon tetrachloride) at which the solid−fluid potential energy is zero, then the accessible pore width is (assuming carbon tetrachloride sitting as a tripod on the graphitic surface)

$$H' = H - 2z_0 + \frac{2}{3}\sigma^{(C,Cl)} + \sigma^{(C,C)} \tag{5}$$

where H is the physical pore width. The local density as a function of distance from the surface is defined as:

$$\rho(z) = \langle \Delta N(z) \rangle / L_x L_y \Delta z \tag{6}$$

where $\Delta N(z)$ is the number of molecules whose centers of mass are located in the segment having boundaries at z and $z + \Delta z$. In the 3D plot of local density distribution, the local density is calculated from

$$\rho(z,\theta) = \langle \Delta N(z,\theta) \rangle / L_x L_y \Delta z \sin\theta \Delta\theta \tag{7}$$

where $\Delta N(z,\theta)$ is the number of molecules whose centers of mass are located in the segment having boundaries z, $z + \Delta z$, and the angle between the vector joining the carbon atom and one of the chlorine atoms and the z direction falls between θ and $\theta + \Delta\theta$. This plot of $\rho(z, \theta)$ vs z and θ allows us to evaluate the preferential orientation of the molecules located at various distances from the wall surface. An angle of 0 means that the molecule lies as a tripod configuration with the base of this tripod formed by the three chlorine atoms, while a value of π means that the molecule takes the inverted tripod configuration.

Experimental data of carbon tetrachloride on graphitized thermal carbon black are available from Machin and Ross,[1] Avgul et al.,[2] and Pierce.[3] These data cover a wide range of temperatures, and this makes these sets of data suitable for the testing of the potential model. Figure 4 shows the experimental data of Machin and Ross as the surface excess vs pressure, while Figure 5 presents the data of Pierce. For comparison, we show in Figure 5 as dashed lines the adsorption isotherms of Machin and Ross at 248 and 273 K. The first observation that we can derive from these two sets of isotherms is that the data of Machin

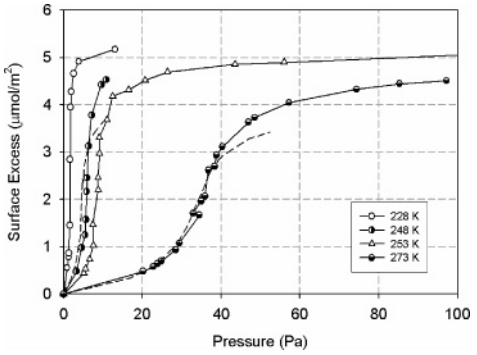

Figure 5. Composite experimental data of Pierce[3] at various temperatures.

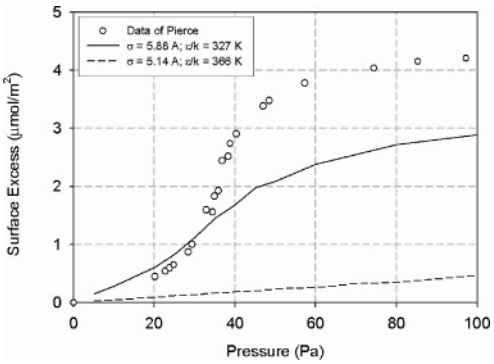

Figure 6. Adsorption isotherm of carbon tetrachloride at 273 K (circles: experimental data; solid line: GCMC results with Monchik and Mason 1C-potential model; dashed line: GCMC results with Radhakrishnan 1C-potential model).

and Ross seem to show lower monolayer coverage concentration, about 4 μmol/m^2, while those of Pierce seem to indicate a higher value of about 5 μmol/m^2. The projection area of carbon tetrachloride was estimated to be 37 Å^2 (Avgul and Kiselev[6]), and this gives a monolayer concentration of 4.5 μmol/m^2. Interestingly, this falls between the two values observed with the set of data of Machin and Ross and that of Pierce. We will consider this point later, but at the meantime, let us start with the analysis of the data. From the data presented by these authors, we select the following temperatures for our analysis, 323, 298, 273, 253, 248, and 228 K. The last two temperatures are below the triple point. The vapor pressures (in Pa) of these temperatures are calculated from the following equation, $P_0 = \exp[C_1 + C_2/T + C_3 \ln T + C_4 T^{C_5}]$, where the constants C's are taken from Perry.[24] These values are 41.367, 15.111, 4.420, 1.339, 0.959, and 0.2114 kPa for 323, 298, 273, 253, 248, and 228 K, respectively. The last two values are extrapolated values because the last two temperatures are below the triple point.

Performance of Simpler 1C-LJ Models. Before discussing the performance of the five-site model, we consider the applicability of the one-site models in the prediction of adsorption isotherms. We select three sets of molecular parameters. The first set is proposed by Radhakrishnan et al.,[25] $\sigma = 5.14$ Å, $\epsilon/k = 366$ K. These parameters were fitted to the bulk properties of solid−liquid coexistence. Another set used by Suzuki et al.[26,27] are $\sigma = 5.88$ Å, $\epsilon/k = 323$ K, and these are taken from the viscosity measurement. The last model is proposed by Monchik and Mason,[28] also taken from the gas viscosity. The molecular parameters are $\sigma = 5.88$ Å, $\epsilon/k = 327$ K, which are very close to the values used by Suzuki et al. These models cannot describe any isotherms of carbon tetrachloride at all, as exemplified in Figure 6 for 273 K. This has also been observed by Lane et al.[29] Therefore, if these models are used to describe adsorption

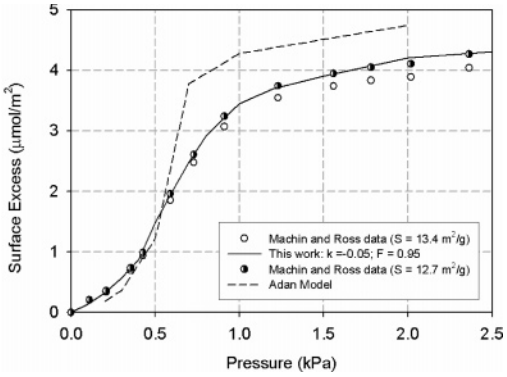

Figure 7. Adsorption isotherm of carbon tetrachloride on GTCB at 323 K (circles: data of Machin and Ross, using a surface area of 13.4 m^2/g; half-filled circles: data of Machin and Ross, using a surface area of 12.7 m^2/g; dashed line: GCMC results obtained with the Adan potential model; solid line: GCMC results using the potential model developed in this work).

in pores, they would incorrectly describe the adsorption isotherms. This is exactly what has been done in Radhakrishnan et al. and Suzuki et al.'s work, and therefore, the conclusions derived from these works might not be valid.

323 K Isotherm Data. First, we take the highest temperature set of data (323 K) of Machin and Ross,[1] and Figure 7 shows the comparison between the data and the GCMC simulation results. To illustrate how the improper potential model results in poor performance in the description of adsorption isotherm, we use the Adan model in the GCMC, and the results of this simulation are shown in Figure 7 as the dashed line. It is seen that the agreement between the data and the GCMC simulation results of the Adan model is very poor. This is the direct consequence of the large value of the well depth of the chlorine atom and the underprediction of the saturation vapor pressure.

Next, we apply the potential model developed in this paper. In the GCMC simulation, we include the surface mediation on the fluid−fluid interaction between particles close to the surface. This effect of surface mediation has been tested for a number of simple gases by Do and co-workers.[30−34] In the case of noble gas family, we have shown that the degree of surface mediation increases linearly with the polarizability.[32] It is lowest for neon and greatest for xenon. Carbon tetrachloride has greater polarizability than noble gases, so one would expect the surface mediation to occur for this adsorbate. This surface mediation comes about because, when two fluid particles are close to the surface, they are no longer surrounded by particles of the same type, but rather they are bound by molecules of the same type above and by carbon atoms of the surface below. Thus, it is expected that the intermolecular interaction between two fluid particles close to the surface is different from that when they are far away from the surface. It is likely that the electric field due to the surface can induce a dipole moment in each particle close to the surface, and because these induced dipoles are on the same plane and pointing in the same direction, there will be repulsion between these induced dipoles, resulting in a reduction in the intermolecular potential energy. In this paper, we propose a simple and empirical means to account for this surface mediation. Whenever a particle is within a distance from the graphite surface (we take it as 6 Å in this paper), the potential energy contribution of this particle to other particles is reduced by F. This means that the potential energy of interaction between particles i and j is calculated from:

$$\varphi_{i,j}^{(a,b)} = F_i F_j \left\{ 4\epsilon^{(a,b)} \left[\left(\frac{\sigma^{(a,b)}}{r_{i,j}^{(a,b)}} \right)^{12} - \left(\frac{\sigma^{(a,b)}}{r_{i,j}^{(a,b)}} \right)^{6} \right] \right\} \qquad (8)$$

where $F_i = F$ if particle i is in the region close to the surface, otherwise it is equal to unity. The same is applied to the particle j. Having this, we simulate the adsorption isotherm by using GCMC and find that the optimal value for F is 0.95. This means that strength of fluid−fluid interaction for each particle close to the surface is reduced by 5%. The results of this simulation are shown as a solid line in Figure 7. The description is good with an exception that the simulation results slightly overpredict the experimental data. The surface area used in their data is 13.4 m^2/g, the value of which was obtained with the BET plot with argon being the probe molecule[35] (projection area is taken to be 13.6 $Å^2$). It is known that the BET surface area depends on the molecular probe as well as the pressure range over which the BET linearized plot is carried out. If we reduce the surface area by 5% to 12.7 m^2/g, it is seen that the GCMC results with our potential model agree very well with the data. We shall come back to this point later when we analyze data at lower temperatures. The data of Machin and Ross at 323 K is restricted to the monolayer coverage, and the maximum value of pressure in the Machin and Ross data is well below the vapor pressure. To test the potential model, we apply it against the data of Avgul and Kiselev at 293 K. The pressure range covered by these authors extends up to 10.2 kPa (reduced pressure of about 0.7), at which there are about three layers that are formed on the surface.

293 K Data of Isotherm and Isosteric Heat (Avgul et al.[2]). The only set of data that extends into the multilayer region is that of Avgul et al.[2], who obtained an isotherm at 293 K. The data are shown in Figure 8 as open circles, while the simulation results are shown as a solid line. The best agreement between the results and the data is achieved with the surface mediation factor of 0.95, which is exactly the same as that obtained earlier for 323 K. To get the correct Henry constant at low pressure, the solid−fluid binary interaction is found to be −0.04, that is, the solid−fluid well depth is 4% greater than the value calculated from the Lorentz−Berthelot mixing rule.

Because these data are extensive and the isosteric heat was reported by the author, we computed the isosteric heat from the GCMC simulation and the results are shown in Figure 9 as the solid line. The experimental data of Avgul et al. are presented as open circles. First, we see that the agreement between the simulation results and the experimental data is very good. The simulation results describe correctly the rise of isosteric heat in the submonolayer coverage, indicating that the fluid−fluid interaction is correctly accounted for. This also implies that the surface mediation is properly described; otherwise the isosteric heat would have increased faster had we not accounted for this effect. Also shown in this figure are the contribution of solid−fluid interaction (dashed−dotted line) and that of fluid−fluid interaction (dashed line) to the isosteric heat. The contribution of solid−fluid interaction shows a small decline in the submonolayer coverage, and this is due to the slight change in the orientation of carbon tetrachloride with loading. At very low loadings, carbon tetrachloride adopts the tripod configuration, and when loading is increased, some molecules will adopt the orientations other than the tripod in order to maximize the fluid−fluid interaction. We will show the orientations of particle in the next section.

273 K Isotherm Data. Next, we consider the experimental data at 273 K, and for this temperature, we have the data of Pierce and also that of Machin and Ross. These two sets of

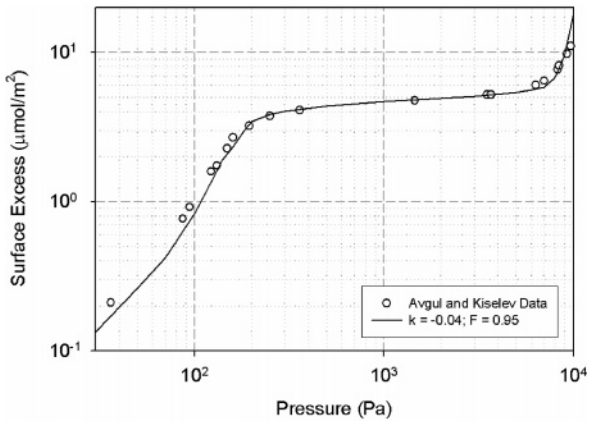

Figure 8. Adsorption isotherm of carbon tetrachloride on GTCB at 293 K (circles: data of Avgul et al.; solid line: GCMC results with the potential model developed in this work, $k_{sf} = -0.04$ and $F = 0.95$).

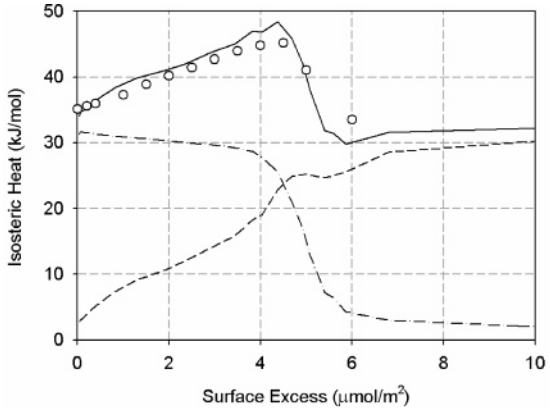

Figure 9. The isosteric heat vs loading (circles: experimental data; solid line: GCMC simulation results; dashed−dotted line: contribution of solid−fluid to the isosteric heat; dashed line: contribution of fluid−fluid to the isosteric heat).

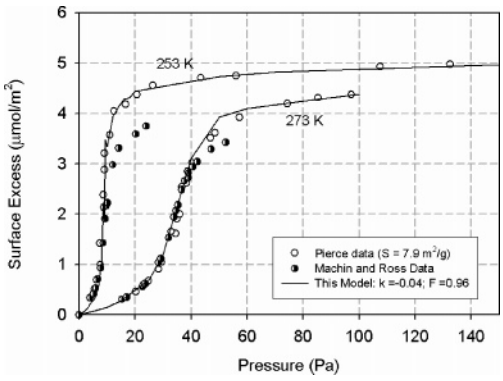

Figure 10. Adsorption isotherm of carbon tetrachloride on graphitized thermal carbon black at 273 and 253 K (unfilled circles, data of Pierce, and half-filled circles are from data of Machin and Ross).

data agree well at low pressures up to about 30 Pa, at which the inflection point in the adsorption isotherm is observed (Figure 10). The concave shape of the isotherm for pressures less than 30 Pa is due to the very strong fluid−fluid interaction of carbon tetrachloride. So what is the reason for the disagreement between these two sets of data for pressures greater than about 40 Pa, that is, into the region where the first layer is being completed?

The data of Pierce and that of Machin and Ross are considered in the framework of GCMC simulation to address the following questions: (1) why are the experimental data very different even though it was reported that the two carbon blacks used by these authors are very homogeneous? (2) Why are the monolayer coverage concentrations obtained from these two sets are distinctly different? First, let us consider briefly the details behind these experimental data. The data of Pierce was obtained with a Sterling MT (3100) with a N_2−BET surface area of 7.65 m^2/g (the projection area of nitrogen was taken to be 16.2 $Å^2$), while and that of Machin and Ross used the P-33 (2700), whose BET surface area obtained with an argon probe is 13.4 m^2/g (the argon projection area was taken to be 13.6 $Å^2$). These two graphitized thermal carbon black samples are known to be very homogeneous.

We see that the Machin and Ross data clearly indicates a lower monolayer coverage concentration than the data of Pierce. It must be remembered that these values of surface excess depend on the choice of the surface area. Pierce used the N_2−BET surface area, while Machin and Ross used the Ar−BET surface area. The projection areas employed by these authors are 16.2 and 13.8 $Å^2$ for nitrogen and argon, respectively. Therefore, the reported experimental surface excess depends on the method used (in their cases, BET) and the value of the molecular projection area.

By using our potential model suggested in this paper, we find that the binary interaction parameter is −0.015 and the reduction factor is 0.95. The GCMC simulation results are consistently above the Machin and Ross data, and for their data to agree with the GCMC simulation results, their BET surface area must be decreased from 13.4 to 10 m^2/g. This decrease is quite significant, and it is hard to attribute this to the incorrect value obtained by the BET method. Let us pause momentarily and discuss the Pierce experimental data. We find that the GCMC simulation results agree well with Pierce data, and this suggests a number of points. First, the Machin and Ross data might not be accurate enough. Second, the simulation results agree with the Pierce data, where an N_2 surface area was used in the calculation, and this suggests that the value of 7.65 m^2/g of the surface area is reliable. As a matter of fact, if we increase the surface area of the sample used by Pierce from 7.65 to 7.9 m^2/g, the agreement between the simulation results and the data is excellent. However, in the analysis of his data, Pierce used the Hill−de Boer equation to fit the portion of the data (fractional loading is less than 0.5); he found that the agreement between the theoretical equation and this limited set of data is possible only when he adjusted the surface area from 7.65 to 9.1 m^2/g. This represents a 20% increase in the surface area so that the Hill-de Boer equation can match the portion of the experimental data! Because the data of this region are too restricted and the validity of the Hill−de Boer (HdB) equation depends on the assumption that the adsorbed phase behaves as a two-dimensional gas governed by van der Waals equation of state, the derivation of a surface area of 9.1 m^2/g by using the HdB equation over a very limited range of data ($\theta < 0.5$) does not carry sufficient weight. So we conclude that the derivation of the surface area of 9.1 m^2/g was wrong and it is an artifact of choosing the inappropriate tool (in their case, the HdB equation) in the analysis. From what we have obtained with the GCMC simulation results, the surface area of 7.9 m^2/g is supported. Indeed it is hard to imagine why a value of surface area is obtained for one molecular probe and a quite different value is derived using another probe. Although there are explanations that have been put forward by Pierce, such is not justified for the 20% difference in the area.

Next, we would like to show the orientation of carbon tetrachloride. Figure 11 shows the 3D local density distribution at 40 Pa vs distance from the surface and angle θ. At this

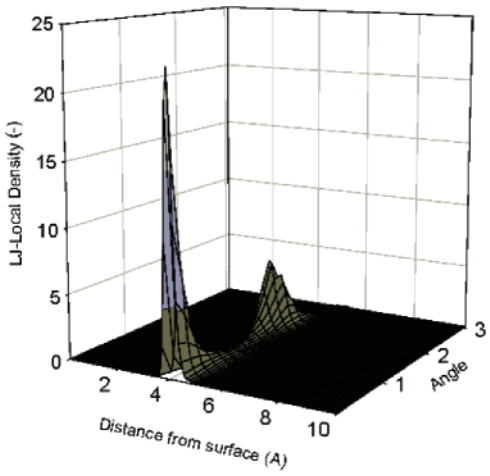

Figure 11. Three-dimensional local density distribution vs distance from the surface and the angle θ, which is formed between the vector pointing from the carbon atom to one of the chlorine atoms and the normal vector from the surface.

pressure, about 70% of the surface is covered with molecules. We see in this figure that most of carbon tetrachloride takes the tripod configuration, while some take a slant orientation (2 rad), which is closer to the inverted tripod configuration (π radian).

253 K Isotherm Data. To further resolve the discrepancy of the difference in the two sets of data (one from Pierce and the other from Machin and Ross) in the region of monolayer coverage, we consider the isotherm data at a lower temperature, 253 K. The experimental results of Pierce and those of Machin and Ross are shown in Figure 10. Like the previous case of 273 K, we see that the data of Machin and Ross and that of Pierce deviate from each other when the monolayer coverage is being reached. This difference can be resolved with the aid of the GCMC simulation, the results of which are also shown in Figure 10 as the solid line. In this simulation, we find that the binary interaction parameter is -0.04 and the surface mediation reduction factor of 0.95. Interestingly, these values are identical to those obtained earlier for 273 K data. Like the previous case of 273 K, we find that the GCMC results agree very well with the data of Pierce, confirming that (a) surface mediation is important and the surface mediation reduction factor is a constant, independent of temperature, and (b) the binary interaction parameter is -0.04 and is independent of temperature, and so is the surface mediation reduction factor.

248 K Isotherm Data. Let us now test this with isotherms at temperatures below the bulk triple point of carbon tetrachloride (which is 250.3 K). The isotherms of Pierce and Machin and Ross at 248 K are shown in Figure 12. The first observation is that these two data substantially disagree with each other, and the monolayer coverage of Machin and Ross is significantly lower than that of Pierce. Moreover, the onset of adsorption is sooner in the case of Machin and Ross data.

We carry out the simulation and the simulation results with $k_{sf} = -0.04$ and F = 0.96 are shown in Figure 12 as the solid line. Again, it is seen that the GCMC results agree with the Pierce data far better. This suggests that the Machin and Ross data are in doubt. Let us briefly discuss the possible failure of Machin and Ross data at this low temperature, 248 K. Like before, the data of Machin and Ross data for the monolayer coverage concentration are lower than the Pierce data and the value obtained from the simulation, and this has been explained by the reason that the surface area of Machin and Ross is overestimated. Even with this correction for the surface area,

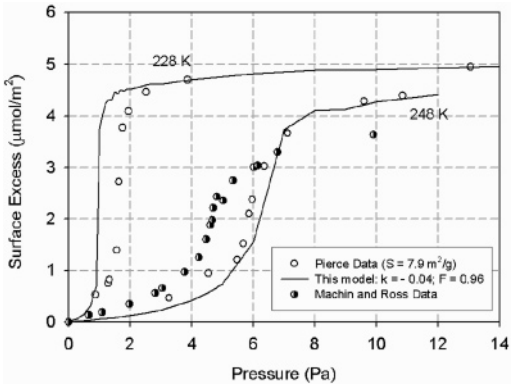

Figure 12. Adsorption isotherms of Pierce (unfilled circles) and Machin and Ross (half-filled circles) at 228 and 248 K. The GCMC results are presented as solid line.

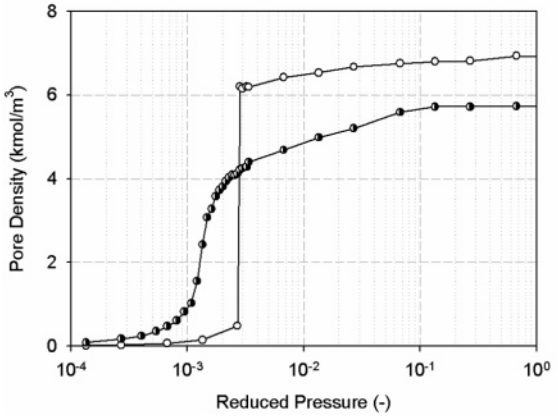

Figure 13. Comparison between the adsorption isotherms in 14.4 Å slit pore at 340 K. The solid line with open circles is from the five-site potential model and the solid line with half-filled circles is from the one-site potential model.

the data of Machin and Ross still show an onset of adsorption at a pressure lower than that observed in the Pierce data and also in the GCMC simulation results. This point has been addressed by Pierce, and it is associated with the reliability of the measurement of very low pressure. It is likely that the pressure of Machin and Ross is wrong because they used the McLeod gauge, and the streaming of mercury could affect the pressure reading. Pierce overcame this problem by using the diaphram gauge, and this is expected to be more reliable than the McLeod gauge.

228 K Data. As another test to justify the model against data below the triple point, we chose the adsorption isotherm at 228 K of Pierce. This is even further away from the triple point. The experimental data and the GCMC results are shown in Figure 12. We see that the GCMC simulation result agrees well with the data at very low pressure and it describes correctly the monolayer coverage concentration. However, it fails to describe the onset of adsorption. The model predicts the onset at about 1 Pa, while the experimental data occurs at about 1.7 Pa. It is not possible to explain for this difference. It could be due to the deficiency of the potential model at temperatures below the triple point, or it could be due to the error in the pressure measurement, as this pressure is a very low pressure.

Having studied the adsorption on an open surface where the packing effect is not manifested, we now consider the adsorption in slit pores.

3.3. Adsorption in Slit Pores. Adsorption of carbon tetrachloride in slit pores has been well studied by Kaneko and co-

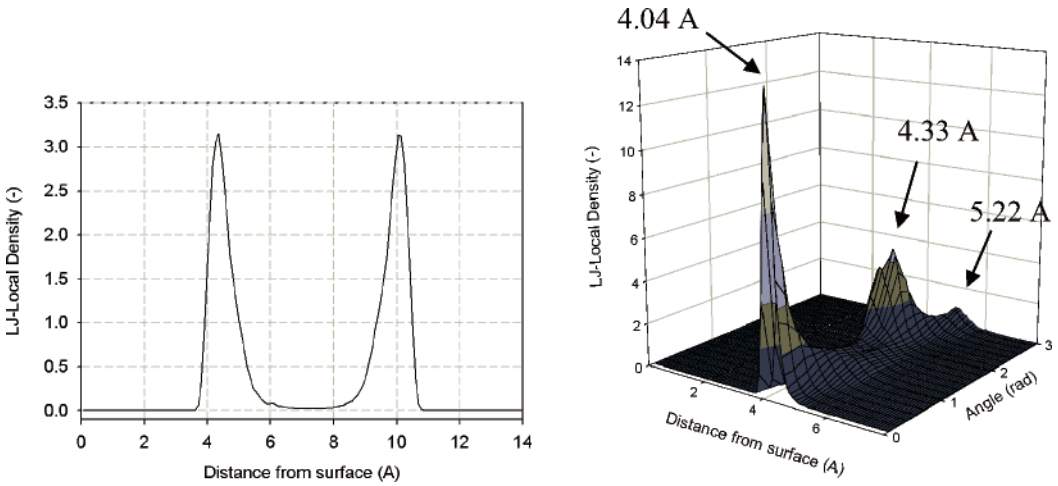

Figure 14. (a) Two-dimensional local density distribution vs distance from the surface at 75 kPa in 14.4 Å; (b) 3D local density distribution vs distance from the surface and the angle θ.

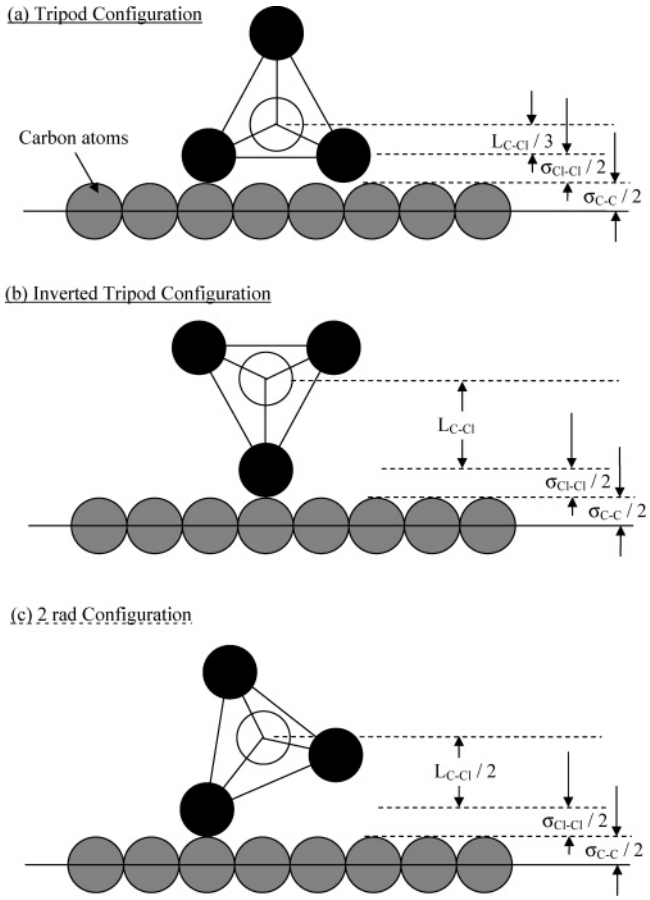

Figure 15. (a) Tripod configuration; (b) inverted tripod configuration; (c) 2 rad configuration.

workers.[25−27,36−37] They used the 1C-LJ model in the description of adsorption isotherm to study the packing effects as well as the elevation of freezing point. In Figure 13, we show the adsorption isotherms in 14.4 Å slit pore (this value of pore size is used previously by Kaneko et al.), using the 1C-LJ model and the five-site potential model developed in this paper. It is clearly seen that these two isotherms are substantially different, and this comes as no surprise because we have shown earlier that the 1C-LJ potential model is not a good choice in the description of adsorption on graphitized thermal carbon black. Therefore, we can draw a conclusion about the inadequacy of the 1C-LJ model in the description of isotherms in slit pores. Although we only show here the difference between the five-site potential model and the one-site model, the same is also observed for other pore sizes as well. This means that the pore size distribution of a porous solid can have significant role in the prediction of the adsorption isotherm.

The local density distribution in this pore is shown in Figure 14a. There are two layers that can be accommodated in this pore. The orientation of carbon tetrachloride can be derived by studying the three-dimensional plot of the local density vs distance from the wall and the angle θ (Figure 14b). Like the case of a surface, most of particles take the tripod configuration, but we see a greater amount of particles taking other configurations.

By analyzing this 3D plot of density distribution (Figure 14b), we see that those molecules with tripod configuration have their centers of mass about 4.04 Å from the surface and those with inverted tripod configuration have a distance of about 5.22 Å. The second major peak occurs at about 2 rad (∼120°) and the distance where this occurs is 4.33 Å. Let us explore this from a geometrical point of view to learn about the way carbon tetrachloride packs inside this 14.4 Å slit pore.

First, let us consider the tripod configuration (Figure 15a). The distance between the COM of the particle and the base passing through the centers of three chlorine atoms is one-third of the carbon−chlorine bond length, which is $L_{C-Cl}/3 = 1.766/3 = 0.589$ Å. The half-collision diameter of chlorine is $\sigma_{Cl-Cl}/2 = 3.5/2 = 1.75$ Å, and half of the collision diameter of carbon is $\sigma_{C-C}/2 = 3.4/2 = 1.7$ Å. Thus, if this tripod sits tightly on the carbon surface, the distance between the surface and the COM of the particle is

$$L_{C-Cl}/3 + \sigma_{Cl-Cl}/2 + \sigma_{C-C}/2 = 0.589 + 1.75 + 1.7 = 4.04 \text{ Å}$$

and this is exactly what we see in the 3D plot of density distribution.

For the inverted tripod configuration, the distance between the COM of a particle and the carbon surface is $L_{C-Cl} + \sigma_{Cl-Cl}/2 + \sigma_{C-C}/2 = 1.766 + 1.75 + 1.7 = 5.216$ Å (Figure 15b), which is the distance that we see in Figure 16b. Last, the second major peak occurs at an angle of 120°, and the COM is at a distance of 4.33 Å from the surface. For this case, the carbon tetrachloride sits on the surface with an angle of 60°, and the distance is the sum of $L_{C-Cl}/2 + \sigma_{Cl-Cl}/2 + \sigma_{C-C}/2 = 1.766/2 + 1.75 + 1.7 = 4.33$ Å (Figure 15c).

What is observed in Figure 14b is that most particles have the tripod configuration, which is the most energetic configu-

ration. The inverted tripod configuration is entropic-favorable, but it is not energetic-favorable. To balance between this entropic factor and the enthalpic factor, particles will adopt the configuration with an angle of 120° (2 rad). This contributes the second major peak observed in the 3D density distribution of Figure 15b.

4. Conclusions

We have presented in this paper a comprehensive simulation study of adsorption of carbon tetrachloride on graphitized thermal carbon black and in graphitic slit pores. The various five-site models proposed in the literature are not adequate in the description of adsorption of carbon tetrachloride on graphitized carbon black, and this is due to their inability in correctly describing the vapor−liquid equilibria, especially the vapor pressure. By using the Gibbs ensemble Monte Carlo simulation, we have derived the optimal molecular parameters for a five-site model for carbon tetrachloride. This model is tested against adsorption data at various temperatures to show its potential. We have found that the surface mediation is important, and the fluid−fluid interaction among molecules in the first layer close to the surface must be reduced by 4%. This is expected because of the high polarizability of chlorine. It is concluded that the correct choice of model is important. We would like to add that no one-site model can correctly describe the experimental data, highlighting the importance of the five-site potential model of carbon tetrachloride. Besides the use of the correct potential, the quality of the data is also equally important. Among the various experimental data that we have tested, we have found that the data of Avgul et al.[2] and that of Pierce[3] are good while the data of Machin and Ross[1] is questionable. Simulations were also carried out to study the packing effects and the elevation of freezing point in graphitic slit pores. Again, the choice of the potential model is important in the analysis of these factors.

Acknowledgment. This work is supported by the Australian Research Council.

References and Notes

(1) Machin, W.; Ross, S. *Proc. R. Soc. London, Ser. A* **1962**, *265*, 455.
(2) Avgul, N. N.; Kiselev, A. V.; Lygina, I. A.; Mikhailova, E. A. *Izv. Akad. Nauk SSSR, Otd. Akad. Nauk* **1962**, 769.
(3) Pierce, C. *J. Phys. Chem.* **1968**, *72*, 1955.
(4) Isirikyan, A. A.; Kiselev, A. V. *J. Phys. Chem.* **1961**, *65*, 601.
(5) Carrott, P. J. M.; Ribeiro Carrott, M. M. L.; Cansado, I. P. P.; Nabais, J. M. V. *Carbon* **2000**, *38*, 465.
(6) Avgul, N.; Kiselev, A. V. *Chem. Phys. Carbon* **1970**, *6*, 1.
(7) Belyakova, L. D.; Kiselev, A. V.; Kovaleva, N. V. *Russ. J. Phys. Chem.* **1968**, *42*, 1204.
(8) Crowell, A.; Young, D. *Trans. Faraday Soc*. **1953**, *49*, 1080.
(9) Crowell, A. *J. Chem. Phys*. **1957**, *26*, 1407.
(10) Crowell, A.; Steele, W. A. *J. Chem. Phys*. **1961**, *34*, 1347.
(11) Gardner, L.; Kruk, M.; Jaroniec, M. *J. Phys. Chem. B* **2001**, *105*, 12516.
(12) Graham, D. *J. Phys. Chem*. **1957**, *61*, 1310.
(13) Graham, D. *J. Phys. Chem*. **1962**, *66*, 1815.
(14) Norman, G. E.; Filinov, V. S. *High Temp*. **1969**, *7*, 216.
(15) Frenkel, D.; Smit, B. *Understanding Molecular Simulation*; Academic Press: New York, 2002.
(16) Nicholson, D.; Parsonage, N. *Computer Simulation and the Statistical Mechanics of Adsorption*; Academic Press: London, 1982
(17) McDonald, I. R.; Bounds, D. G.; Klein, M. L. *Mol. Phys.* **1982**, *45*, 521.
(18) Adan, F.; Banon, A.; Santamaria, J. *Chem. Phys. Lett*. **1984**, *107*, 475.
(19) Steele, W. A. *Surf. Sci*. **1973**, *36*, 317.
(20) Steele, W. A. The Interaction of Gases with Solid Surfaces. Topic 14. *International Encyclopedia of Physical Chemistry and Chemical Physics*; Pergamon Press: Elmsford, NY, 1974; Vol. 3.
(21) Panagiotopoulos, A. Z. *Mol. Phys*. **1987**, *61*, 813.
(22) Hill, T. *Statistical Mechanics*; Dover: New York, 1956.
(23) Kaneko, K.; Cracknell, R.; Nicholson, D. *Langmuir* **1994**, *10*, 4606.
(24) Perry, C. *Chemical Engineering Handbook*; McGrawHill: New York, 1998.
(25) Radhakrishnan, R.; Gubbins, K. E.; Watanabe, A.; Kaneko, K. *J. Chem. Phys.* **1999**, *111*, 9058.
(26) Suzuki, T.; Kaneko, K.; Gubbins, K. *Langmuir* **1997**, *13*, 2545.
(27) Suzuki, T.; Iiyama, T.; Gubbins, K. E.; Kaneko, K. *Langmuir* **1999**, *15*, 5870.
(28) Monchick, L.; Mason, E. A. *J. Chem. Phys.* **1961**, *35*, 1676.
(29) Lane, J.; Quint, G. L.; Spurling, T. H. *Aust. J. Chem.* **1983**, *36*, 1733.
(30) Do, D. D.; Do, H. D.; Kaneko, K. *Langmuir* **2004**, *20*, 7623.
(31) Do, D. D.; Do, H. D. *Adsorpt. Sci. Technol*. **2005**, *23*, 267.
(32) Do, D. D.; Do, H. D. *Fluid Phase Equilib.* **2005**, *236*, 169.
(33) Do, D. D.; Do, H. D. *Mol. Simul*. **2005**, *31*, 651.
(34) Do, D. D.; Do, H. D. *J. Colloid Interface Sci*. **2005**, *287*, 432.
(35) Ross, S.; Olivier, J. *J. Phys. Chem.* **1961**, *65*, 608.
(36) Iiyama, T.; Suzuki, T.; Kaneko, K. *Chem. Phys. Lett*. **1996**, *259*, 37.
(37) Iiyama, T.; Nishikawa, K.; Suzuki, T.; Otowa, T.; Hijiriyama, M.; Nojima, Y.; Kaneko, K. *J. Phys. Chem. B* **1997**, *101*, 3037.